Environmental and Experimental Botany 201 (2022) 104970

Contents lists available at ScienceDirect

Environmental and Experimental Botany

journal homepage: www.elsevier.com/locate/envexpbot

Molecular basis of intraspecific differentiation for heavy metal tolerance in the copper moss *Scopelophila cataractae*

M. Teresa Boquete [a,b,c,*], Marc W. Schmid [d], Niels C.A.M. Wagemaker [e], Sarah B. Carey [f], Stuart F. McDaniel [f], Christina L. Richards [c,g], Conchita Alonso [a]

[a] Department of Evolutionary Ecology, Estación Biológica de Doñana, CSIC, Sevilla, Spain
[b] Area of Ecology, Department of Functional Biology, Universidade de Santiago de Compostela, Spain
[c] Department of Integrative Biology, University of South Florida, Tampa, FL, USA
[d] MWSchmid GmbH, Glarus, Switzerland
[e] Faculty of Science, Raboud University, Nijmegen, the Netherlands
[f] University of Florida, Gainesville, FL, USA
[g] Plant Evolutionary Ecology group, University of Tübingen, Tübingen, Germany

ARTICLE INFO

Keywords:
Abiotic stress response
DNA methylation
Epigenetics
Metallophyte moss
Phenotypic variation
Reduced representation bisulfite sequencing
RNA sequencing

ABSTRACT

The remarkable capacity of bryophytes to tolerate extremely challenging abiotic conditions allows us to enhance our understanding of the diversity of molecular mechanisms involved in plant stress response. Here, we used next generation sequencing to study DNA methylation and gene expression changes in plants from four populations of the metallophyte moss *Scopelophila cataractae* experimentally exposed to either Cd or Cu. These populations previously showed differences in tolerance to both metals, so here, we aimed to investigate the molecular basis of this phenotypic differentiation. We found no evidence of genetic differentiation among the populations studied. The epigenetic data, however, showed limited but significant population-specific changes in DNA methylation in response to both metals. Exposure to acute Cu stress in the laboratory led to the downregulation of genes involved in heavy metal tolerance in both the more and the less tolerant populations, but this response was quantitatively higher in the most tolerant. We propose that chronic exposure to varying levels of heavy metals in the field led to potentially non-genetically-based intraspecific differentiation for heavy metal tolerance in *S. cataractae*. The most tolerant plants invested more in constitutive protection and were more efficient at entering a conservative state when faced with acute Cu stress.

1. Introduction

Heavy metals are among the most hazardous pollutants to living organisms due to their high toxicity and persistence in the environment (Ali et al., 2019; He et al., 2005; Kanawade et al., 2010; Rhind, 2009). Multiple studies have shown that heavy metals damage the cell membrane system and negatively affect plant development, growth, and reproduction (Brown and Wells, 1990; Devi and Prasad, 1999; Guschina and Harwood, 2002; Janicka-Russak et al., 2008), generate reactive oxygen species (ROS) (Boominathan and Doran, 2002; Shahid, 2014), and may alter the structure of essential plant biomolecules (Assche and Clijsters, 1990; Küpper et al., 2002; Küpper et al., 2002; Tan et al., 2010). Still, some species have adapted to living in heavy metal-enriched environments, and are able to survive and accumulate concentrations of heavy metals that greatly exceed the tolerance limits of most other plants (Verbruggen et al., 2009; Krämer, 2010; Papadopulos, 2021).

Metal tolerant species often rely on the enhanced expression of genes related to heavy metal homeostasis – i.e. transport, chelation, and sequestration of metals – relative to closely related non-tolerant ones (Becher et al., 2004; Gao et al., 2013; Halimaa, 2014; Meier, 2018; Pence, 2000; van de Mortel, 2006). Thus, constitutive overexpression of heavy metal homeostasis-related genes (e.g. ABC metal transporters and enzymes involved in oxidative stress relief (Halimaa, 2014; Meier, 2018)) is associated with differences between tolerant and non-tolerant plants (but see (Hanikenne, 2008; Talke et al., 2006) for the contribution of gene copy number variation). Yet, the regulatory mechanisms determining the differences in gene expression are still poorly

* Correspondence to: Area of Ecology, Department of Functional Biology, Universidade de Santiago de Compostela, Santiago de Compostela, Spain.
E-mail address: teresa.boquete@usc.es (M.T. Boquete).

https://doi.org/10.1016/j.envexpbot.2022.104970
Received 13 April 2022; Received in revised form 13 June 2022; Accepted 14 June 2022
Available online 18 June 2022

understood. Gene expression in eukaryotic genomes is, in part, tightly regulated by epigenetic mechanisms, the set of chromatin modifications that control chromatin structure, and thus, the accessibility of the transcriptional machinery to genes (Bartee et al., 2017; Li et al., 2007). In plants, epigenetic mechanisms, such as DNA methylation, histone modifications, and small non-coding RNAs, are known to regulate gene expression changes in response to developmental and environmental cues (Gehring et al., 2009; Lang, 2017; Rathore et al., 2020; Sanchez and Paszkowski, 2014; Tsuji et al., 2006; Zhang et al., 2011). Based on this evidence, epigenetic mechanisms are considered to be potentially important regulators of plants response to stress.

So far, experimental evidence on the contribution of epigenetic mechanisms to plant heavy metal tolerance has shown that DNA methylation could have a direct protective role. For example, metal tolerant plants like *Arabidopsis halleri* - in response to Cd - and *Noccaea caerulescens* - in response to Ni showed hypermethylation of DNA and no heavy metal-induced DNA damage (Galati, 2021; Gullì et al., 2018). Non-tolerant species like the moss *Physcomitrium patens*, however, showed overall DNA hypomethylation and significant signs of DNA strand breaks in response to Mn (Ghosh et al., 2019). Studies employing anonymous DNA methylation markers or immunolabelling techniques reported DNA hypermethylation in response to exposure to high Al levels in wheat (*Triticum aestivum*) (Pour et al., 2019) and maize (Taspinar, 2018), to Pb in maize (*Zea* mays) (Agar, 2014), to Cd in *Posidonia oceanica* (Greco et al., 2012) and *Nicotiana benthamiana* (Xin et al., 2019), and to Cd, Ni and Cr in *Trifolium repens* and *Cannabis sativa* (Aina, 2004). In contrast, DNA hypomethylation was reported in response to Cd in rapeseed (*Brassica napus*) (Filek, 2008) and the red alga *Gracilaria dura* (Kumar et al., 2012), to Al in triticale (x *Triticosecale*) (Bednarek et al., 2017; Niedziela, 2018), to Cu and Zn in *Populus alba* (Cicatelli, 2014), and to low Al levels in wheat (Pour et al., 2019). Epigenetic mechanisms like DNA methylation can thus be modified in response to heavy metal exposure.

More targeted studies have demonstrated that epigenetic changes induced by heavy metals are associated with changes in the expression of genes involved in heavy metal tolerance. For example, work with methylation mutants confirmed that CG and H3K9me2 hypomethylation upstream of the metal responsive metallochaperone, *OsHMP*, was associated with its overexpression and enhanced Cd tolerance in rice (*Oryza sativa*) (Feng et al., 2021). Similar DNA and histone hypomethylation was associated with increased expression of a Cd tolerance factor (*OsCTF*) that enhanced Cd tolerance in rice (Feng, 2020). Other studies used transformation of *Arabidopsis thaliana* with an S-adenosylmethionine synthetase (SAMS) gene, which encodes an enzyme that catalyzes the biosynthesis of SAM, the main methyl group donor for DNA methylation in plants. This transformation conferred Al as well as Cd, Cu, and Zn tolerance to this species (Ezaki et al., 2016). The overexpression of specific heavy metal detoxification transporters in a Pb, Cd, and Zn tolerant variety of wheat has been linked to CG hypomethylation in their promoter region in response to all three metals (Shafiq, 2019). Prolonged Cr exposure during selection of a Cr-tolerant strain of the green alga *Scenedesmus acutus* led to new DNA methylation and expression patterns in protein-coding genes involved in Cr tolerance. MicroRNAs also seem to contribute to plant response to Cr stress in rice (Dubey, 2020), Cd in rice (Ding et al., 2011; Huang et al., 2009) and rapeseed (Huang, 2010; Xie, 2007), and Al, Cd, and Hg in *Medicago truncatula* (Zhou et al., 2008). Finally, some studies showed that DNA methylation changes induced during heavy metal exposure can be transmitted to the offspring in rice (Cong, 2019; Ou, 2012) and *Arabidopsis* (Rahavi et al., 2011) potentially leading to heritable changes in gene expression patterns. Collectively, these data suggest that epigenetic regulation could play an important role in plant responses to heavy metal stress. However, these studies are based on a phylogenetically restricted set of species, largely from the *Brassicaceae* and *Poaceae* (i.e. crops and model plants like *Arabidopsis*), which may not be representative of plants as a whole.

Bryophytes, the sister group to the vascular plants, have long been known for their capacity to tolerate high concentrations of heavy metals in their tissues (Shaw, 1989). Most of what is presently known about their tolerance mechanisms comes from biochemical and physiological studies. Mechanisms such as retention of heavy metals in extracellular wax-like substances (Elvira et al., 2020), sequestration in the cell wall (Konno et al., 2010; Krzesłowska et al., 2009; Krzesłowska and Woźny, 2008; Lang and Wernitznig, 2011), preferential accumulation in specific parts/organs of the leafy plant – i.e. gametophore (Antreich et al., 2016; Boquete et al., 2021; Sabovljević, 2020), or the activation of the ROS scavenging machinery and induction of metal-chelating proteins (Bellini, 2020; Petraglia, 2014), have been reported to mitigate heavy metal stress in bryophytes. However, we lack data about the molecular underpinnings of these anatomical or physiological phenomena. Filling this gap will enable us to test whether the land plants employ conserved pathways to tolerate heavy metal stress, or whether each lineage has evolved novel mechanisms.

In this study, we used a reduced representation bisulfite sequencing technique (hereafter epiGBS (van Gurp, 2016)), and RNA sequencing (RNAseq) to quantify the effect of Cd and Cu exposure on DNA methylation and gene expression in the copper moss *Scopelophila cataractae* (Mitt.) Broth. This species has a high affinity for heavy metal, especially Cu-enriched substrates (Shaw, 1993). In previous work we found differences in Cd and Cu tolerance (defined as the ability to maintain vegetative growth in metal stressed vs. control conditions, *sensu* (Simms, 2000)) in this species that depended on the source of origin (Boquete et al., 2021). Plants collected from the center of a Cu mine had been growing in microhabitats devoid of any vegetation and exposed to higher metal concentrations. These plants were more tolerant of heavy metal treatments in the laboratory. In contrast, plants from the mine edges, were collected from milder, less contaminated microhabitats and were less tolerant of heavy metal treatments. Here we used epigenetic and transcriptomic analyses to identify the mechanisms driving intraspecific differentiation for heavy metal tolerance in *S. cataractae*. Specifically, we addressed the following questions: (1) Are intraspecific differences in heavy metal tolerance in *S. cataractae* driven by genetic differentiation? (2) Does heavy metal exposure affect DNA methylation? (3) What are the main gene expression changes in *S. cataractae* in response to heavy metal exposure? (4) Is there any association between methylation and expression changes? Our results provided evidence for non-genetically-based intraspecific phenotypic differentiation for heavy metal tolerance in this species with the more tolerant plants investing more in constitutive protection mechanisms and being more efficient in entering a conservative state when faced with acute Cu stress.

2. Materials and methods

2.1. Field sampling

We collected plants from four populations of *S. cataractae* (Sc1 to Sc4) in a former copper mine in Silver Hill, North Carolina (USA; 17 N 572397E 3951654 N) in September 2016. We use the term population to refer to physically unconnected and scattered patches of this species (separated by mostly bare soil), even though the distance between these patches was very short (~20 to ~300 m). These populations were exposed to different concentrations of heavy metals in the field: the two growing in the center of the mine (Sc2, Sc3) were exposed to higher concentrations of Cd and Cu than the two growing in microhabitats located at the edges of the mine (Sc1, Sc4) (Boquete et al., 2021). At every site, we sampled gametophytic tissue of *S. cataractae* from several moss patches.

2.2. Common garden experiments

We performed two common garden experiments to test separately

the effect of Cd and Cu on DNA methylation and gene expression in *S. cataractae*. First, we clonally propagated each population in growth chambers at 22 ºC and 16 h light/8 h dark with a light intensity between 80 and 100 μmol m^{-2} s^{-1} for a year (conditions maintained for all experiments). Although we did not specifically test for dehardening/deacclimation for heavy metal stress in plants from this study, we assumed that this should have happened within a year based on the short periods (few days) needed to deacclimate bryophytes for other stresses like desiccation (Hellwege et al., 1994; Pence, 1998) (but see (Stark et al., 2012)). We cleaned individual gametophores with deionized (DI) water and a brush under the dissection microscope, cut them into small pieces with a razor blade, and spread them into 4 × 4 cm pots containing a 2:1 mixture of clay (Turface) and commercial soil. Second, we selected 50–70 gametophores from each lab grown culture, cleaned them with DI water as explained above, cut them into small pieces, and spread them in 4 × 4 cm pots containing a previously autoclaved 2:1 mixture of clay and potting soil. We grew five replicates per population (n = 4) and treatment (n = 3) combination (n = 60 pots in total) for 3 months in a growth chamber watering the pots with DI water every two days. After this period, we applied the treatments by watering the plants every two days with 20 mL of water (controls), or water containing 1 mM Cu (Cu), or 0.1 mM Cd (Cd) (n = 4–5 replicates per population and treatment). After 30 days, we harvested the plants, blotted them with filter paper and made several aliquots that were immediately frozen in liquid N and stored at − 80ºC for DNA methylation and gene expression analyses. Other aliquots of these same samples were used for the phenotypic characterization (Boquete et al., 2021).

2.3. DNA extraction and epiGBS library preparation

We isolated genomic DNA (gDNA) from four *S. cataractae* populations (Sc1, Sc2, Sc3, Sc4) with each exposed to three treatments (control, Cd-treated, Cu-treated) hereafter referred to as groups (n = 12 groups); each group replicated in triplicate (n = 36 samples in total). We followed the cetyltrimethylammonium bromide (CTAB) DNA extraction protocol for recalcitrant plant tissues (https://www.protocols.io/view/high-quality-dna-extraction-protocol-from-recalcit-i8jchun) with small modifications (detailed protocol available in the Supplementary Methods - SMs). We checked the quality of the gDNA with the NanoDrop (Nanodrop™ 8000 Spectrophotometer; Thermo Scientific), and quantified its concentration using the Qubit 3.0 Fluorometric dsDNA BR assay kit (Q32851; Life Technologies). We obtained high quality gDNA for all samples except for one replicate of Sc3 in control conditions, which we did not include in the sequencing library.

We prepared the epiGBS libraries following (van Gurp, 2016). We digested 400 ng of gDNA from each sample with the restriction enzyme *PstI*. Then, we ligated methylated, non-phosphorylated barcoded adapters to both ends of the digested fragments. We concentrated the library using the NucleoSpin™ Gel and PCR Clean-up Kit (12303368, Macherey-Nagel™) and performed a fragment size selection with 0.8x SPRI beads (A63880, Agencourt AMPure XP Beckman coulter). We performed nick translation, bisulfite converted the DNA using the EZ Lightning methylation kit (Zymo Research), and amplified the library with the KAPA HIFI Uracil+ Hotstart Ready Mix (Roche) under the following PCR conditions: initial denaturation step at 95 ºC for 3 min; 20 cycles of 98 ºC for 10 s, 65 ºC for 15 s, and 72 ºC for 15 s; final extension of 72 ºC for 5 min. Finally, we quantified the library using the Qubit dsDNA assay kit, pooled all samples using equimolar concentrations and assessed its quality by analyzing 1 μL on a High Sensitivity DNA chip on an Agilent 2100 Bioanalyzer. The library was sequenced at Novogene (HK) Company Limited in Hong Kong on the Illumina HiSeq X-Ten System (PE-150 bp).

2.4. RNA extraction and RNAseq library preparation

Budget limitations precluded analyzing the full set of samples, so we measured gene expression on a subset of 12 samples including control and Cu-treated plants from two populations that had been exposed to different levels of heavy metals in the field and showed contrasting responses to Cu exposure in the laboratory: one from the center of the mine (Sc3) and one from the edges of the mine (Sc4) (n = 3 replicates per population and treatment). Total RNA was isolated with the RNeasy Plant Mini Kit (74904, Qiagen) following the manufacturer instructions with small modifications (detailed protocol available in the SMs).

We prepared cDNA libraries with the NEBNext® Ultra™ II Directional RNA Library Prep with Sample Purification Beads (E7765S, NEB) following the manufacturer's protocol with 1 μg of total RNA as input material (see detailed protocol in SMs). The University of Florida Interdisciplinary Center for Biotechnology Research on the Illumina HiSeq 3000 performed paired-end sequencing (PE-150) of these libraries.

2.5. Data processing

2.5.1. epiGBS data processing and filtering

We used the pipeline provided by (van Gurp, 2016) with a bug-fix modification (https://github.com/MWSchmid/epiGBS_Nov_2017_fixed) to process the sequencing files (sensu (Mounger, 2021)). First, we created a *de novo* reference from the demultiplexed and quality trimmed sequencing reads. We mapped the reads to the *de novo* reference and performed strand-specific nucleotide (single nucleotide polymorphisms, SNPs) and methylation (single methylation polymorphisms, SMPs) variant calling. We filtered the resulting SNP and SMP files as follows: i) we initially removed SNPs and SMPs without a minimum coverage of 3 (i.e. 3 sequencing reads mapping to each locus) and a maximum coverage equal to the 99th percentile of the read coverage distribution, in at least one replicate sample per group ii) we removed samples lacking more than 20 % of the SNPs or more than 25 % of the SMPs; and iii) after removing these samples from the experimental design, we used the original SNP and SMP dataset and removed SNPs and SMPs without a minimum coverage of 10 and a maximum coverage equal to the 99th percentile of the read coverage distribution in at least one replicate sample per group.

The unfiltered datasets resulting from the epiGBS pipeline consisted of 279,103 SNPs and 22.3 million SMPs across all 35 samples. The first and less strict filtering step resulted in 58,773 SNPs and 290,547 SMPs. During the second step we removed 5 samples with low SNP and SMP coverage which, in general, had a low number of sequencing reads after demultiplexing and quality trimming (Table S1). The last and stricter filtering resulted in 52,513 SNPs and 239,728 SMPs across 30 samples comprising 2–3 replicates per group (Table S1).

We created a final SMP working dataset by removing: i) SMPs with any missing values across all 30 samples to obtain a complete SMP matrix (we discarded 196,039 SMPs); ii) SMPs called on the same cytosine as a SNP (we removed 324 positions); and iii) monomorphic SMPs, i.e. SMPs with a methylation frequency $\leq$ 5 % and $\geq$ 95 % across 95 % (i.e. n = 28) of the samples. We calculated the methylation level at each SMP in each individual sample as the number of reads mapping to one position with methylation divided by the total number of reads mapping to that position. The final matrix, containing only polymorphic SMPs, consisted of 3769 cytosines across 30 samples. Similarly, we removed SNPs with any missing values across all 30 samples; the final SNP working dataset consisted of 23,252 SNPs.

2.5.2. RNA-seq data processing, de novo transcriptome assembly, and transcript abundance estimation

We quality trimmed the raw sequencing reads by removing adaptors and low-quality bases with Trimmomatic v 0.36 (Bolger et al., 2014) with a 4-base sliding window and quality threshold of 25. These reads were used for *de novo* transcriptome reconstruction with Trinity v 2.8.4 (Grabherr, 2011), following the protocol by (Haas, 2013). Then, we clustered highly redundant transcripts, i.e. transcripts with > 95 %

sequence similarity, using CD-HIT v 4.6.6 (Fu et al., 2012), and selected the longest isoform per gene using Trinity's custom script (get_longest_isoform_seq_per_trinity_gene.pl). We assessed the quality of the assembly by mapping the trimmed reads back to the assembly using Bowtie2 v 2.2.9 (Langmead and Salzberg, 2012) and evaluated its completeness by searching for orthologues with BUSCO v 3.1.0 (Simão et al., 2015) using the viridiplantae-odb10 database as a reference (E-value cutoff for the blast alignments: $1e^{-06}$).

We estimated transcript abundance within each individual sample using RSEM (Li and Dewey, 2011) wrapped by scripts included in Trinity (align_and_estimate_abundance.pl). This software first aligns the sequenced reads back to the transcriptome, and then provides read counts and normalized expression values for each transcript in each sample. Finally, we created a count matrix with read counts across all samples.

2.5.3. Annotation of de novo transcriptome assembly

We used the pipeline available within the bioinformatics platform OmicsBox (Götz, 2008; OmicsBox – Bioinformatics Made Easy, 2019) to annotate the *de novo* transcriptome as follows: i) we performed a blast search against the non-redundant protein sequence database (nr v5) (blastx-fast; E-value cutoff: $1e^{-05}$); ii) we retrieved gene ontology (GO) terms for the sequences with blast hits using the gene_info and gene2accession files from the NCBI database, and UniProt IDs using the PSD, UniProt, Swiss-Prot, TrEMBL, RefSeq, GenPept and PDB databases; iii) we annotated the sequences by assigning the most reliable and specific GO terms according to their E-values ($< 1e^{-06}$) and sequence similarities (high scoring segment pair hit coverage cutoff of 80 %) as well as the quality of their annotation using the evidence code for each GO term (1 for experimental evidence, 0.7–0.8 for computational analysis evidence, and 0.5–0.9 for all other evidence types) (Conesa, 2005); iv) in parallel, we searched for matches between our sequences and protein domains and families within the InterPro protein databases and the EggNOG database to annotate predicted orthologues within our query sequences (Huerta-Cepas, 2019); v) we merged the InterPro and EggNOG classifications with the annotation resulting from step (iii).

Additionally, we used RepeatMasker v 4.0 to annotate transposons and repeats in the *de novo* reference genome (obtained with the epiGBS bioinformatics pipeline) using Embryophyta as reference species collection (v.4.0.6 (Smit et al., 2013)) and DIAMOND v 0.8.22 to annotate protein coding genes with the NCBI non-redundant protein sequences database (Buchfink et al., 2015), in order to classify epigenetic variants into different genomic features.

2.6. Statistical analysis

All analyses were performed in R v.3.5.1 (Core and Team, 2018) running under R Studio v.1.2.5019 (RStudio Team, 2019).

2.6.1. Genetic analyses

To determine if the phenotypic differences in tolerance were associated with genetic differences we tested for genetic differentiation among populations of *S. cataractae*. Thus, we performed an analysis of molecular variance (AMOVA) with the function *poppr.amova* in the poppr R package (Kamvar et al., 2014), based on SNPs with no missing values (n = 23,252 SNPs). This function takes a genind object (created with the function *df2genind* from adegenet (Jombart, 2008); ploidy= 1) as dependent variable and population (with 4 levels, n = 7–8 samples per level) as predictor. We assessed the significance of the model using a randomization test with 9999 permutations on the output of the AMOVA (function *randtest* from the ade4 package (Dray and Dufour, 2007)). Additionally, we calculated the likelihood ratio G-statistic to test for significant genetic differentiation among populations (*gstats.glob* function from the hierfstat package (Goudet, 2005) with 9999 permutations). We assessed its significance by comparing the observed statistic with the distribution of the G-statistic on a null dataset where samples were randomly shuffled among populations using the function *samp.between* from hierfstat (9999 repetitions).

We visualized genetic data by means of principal component analysis (PCA) carried out with the function *dudi.pca* (ade4 package) on a scaled and centered allele frequency matrix obtained with the function *scaleGen* (adegenet package).

2.6.2. Epigenetic analyses

We calculated the methylation level at each SMP and individual sample and estimated the mean and standard deviation of DNA methylation per group, for each separate sequence context (i.e. CG, CHG and CHH), and across all contexts, using the complete SMP matrix (n = 43,365 SMPs) as well as the complete and polymorphic SMP matrix (n = 3769 SMPs). All other analyses were performed for each of the two common garden experiments by comparing control vs. Cd-treated and control vs. Cu-treated plants from all four populations using the matrix of complete and polymorphic SMPs.

To evaluate response to each heavy metal, we carried out a distance-based RDA (dbRDA (Legendre and Anderson, 1999)) to test the effect of population (n = 4), treatment (n = 2; C vs. Cd or C vs. Cu), and their interaction on genome wide DNA methylation with the model: epigenetic distance ~ Population * Treatment (function *capscale* in the vegan package (Oksanen, 2020)). This constrained multivariate ordination approach provides an estimate of the amount of variation in epigenetic distances explained by our predictors, as well as the constrained ordination axes (RDA axes) used to visualize the structure of the data in a two-dimensional space. We estimated pairwise epigenetic distances following Wang et al. (2019), where the distance (d_{st}) between any two samples, s and t, was calculated either based on only the level of methylation or including the variance in methylation as follows:

$$d_{st} = \sqrt[2]{\sum_{j=1}^{n}\left\{\frac{1}{2n}\left(x_{sj}^{m} - x_{tj}^{m}\right)^{2} + \frac{1}{2n}\left(x_{sj}^{v} - x_{tj}^{v}\right)^{2}\right\}}$$

Where n is the number of cytosine positions (SMPs); x_{sj}^{m} and x_{tj}^{m} represent the ***methylation level*** of cytosine j in samples s and t respectively; and x_{sj}^{v} and x_{tj}^{v} represent the ***methylation variance*** of cytosine j in samples s and t respectively. The methylation variance (x_{ij}^{v}) was estimated as the squared difference between the methylation level of cytosine j in sample i (x_{ij}^{m}) and the average methylation of cytosine j across all samples in the group to which sample i belongs ($\overline{x}_{j}^{m}$). Using the formula above, we also accounted for the variation in methylation profiles within treatment groups.

We ran separate dbRDA models for each common garden experiment (i.e. C vs. Cd and C vs. Cu) for all sequence contexts together and separately for each sequence context. In each of these cases, we first ran the model using the epigenetic distance matrix calculated using only differences in methylation levels between each pair of samples (using only the left-hand side under the square root of the formula above). Then, we ran the model using the distance matrix calculated from both methylation level and methylation variance (full formula). We tested the overall significance, as well as the significance of each predictor and their interaction using a permutation test with 9999 permutations. We calculated the proportion of total variance explained by our models, adjusted by the number of predictors included in the model (adj. R(He et al., 2005)), with the function *RsquareAdj* (vegan package) which provides a unique adj. R^2 for the full model. We also calculated individual adj. R^2 for each predictor by modeling the effect of each predictor while accounting for the others using partial constrained dbRDA with the following models: i) epigenetic distance ~ Treatment + Condition (Population); ii) epigenetic distance ~ Population + Condition(Treatment); iii) epigenetic distance ~ Population:Treatment + Condition (Treatment) + Condition(Population).

We identified differentially methylated cytosine positions (DMPs) as

cytosines with significant differences in their mean methylation level between control and Cu-treated, and control and Cd-treated plants using the R package DSS (Feng et al., 2014). First, we modeled the methylation frequency at each cytosine position within each group using a beta-binomial distribution with arcsine link function and the formula "~ 0 + group" (function *DMLfit.multifactor*). This transformation proved useful to model DNA methylation because it reduces the heteroscedasticity of the data by stabilizing its variance (Park and Wu, 2016; Zheng et al., 2017). Second, we performed Wald tests to detect differential methylation between groups at each position using the function *DMLtest.multifactor* which reports adjusted p-values by the Benjamini-Hochberg method (i.e. FDR). We considered cytosines to be differentially methylated (i.e. DMPs) when FDR $\leq$ 0.05 and methylation change was $\geq$ 10 %.

2.6.3. Gene expression analysis

We identified differentially expressed transcripts (DETs) between control and Cu-treated plants from Sc3 and Sc4 using edgeR v3.24.3 (Robinson et al., 2010). First, we filtered low count transcripts by removing those with less than 2 cpm (counts per million; i.e. less than 10 counts per transcript) in at least 3 samples to ensure that we kept any transcript that was highly expressed in all three replicates from one group. A total of 23,016 transcripts (7 % of the total) passed this filter and were used in subsequent steps. Second, we fitted the model using the function *glmQLFit* (option robust = TRUE) and tested for DETs using the function *glmTreat*. Transcripts were considered differentially expressed when FDR < 0.001 and expression change was $\geq$ 4-fold ($\log_2$FC $\geq$ 2).

To better understand the changes associated with Cu exposure, we performed a Fisher's exact test (with the FatiGO (Al-Shahrour et al., 2004) package implemented within OmicsBox) on the list of DETs from each population. With this method, we tested for significant differences in the fraction of transcripts annotated with a specific GO term between the DETs list (test set) and the full list of annotated transcripts (reference set). We applied an FDR cutoff of 0.01, and used the "*Reduce to most specific*" option within OmicsBox to remove the more general, less informative, GO terms.

2.6.4. Association between DNA methylation and gene expression changes

To find transcripts that were both differentially methylated and differentially expressed between Cu-treated and control plants, i.e. potential associations between changes in DNA methylation and gene expression, we mapped the *de novo* reference to the *de novo* transcriptome using Blat (Kent, 2002) and intersected IDs of the mapped sequences with the IDs of the lists of DMPs and DETs for each population.

3. Results

For the epiGBS libraries, we recovered 85.8 million reads after demultiplexing. The number of reads per sample averaged 2.5 million and ranged between 0.6 and 4.5 million. Sequenced reads were evenly distributed across all four populations (21.4 $\pm$ 1.7 million reads per population), and across all 12 groups (7.2 $\pm$ 2.1 million reads per group) (Table S1). For the RNAseq libraries, we recovered 101.8 million reads after quality trimming. The number of reads per sample averaged 8.5 million and ranged between 6.9 and 10.2 million (Table S2). As for the epiGBS dataset, the sequencing power was evenly distributed across populations (51.0 and 50.8 million reads for Sc3 and Sc4 respectively), and the four groups (25.5 $\pm$ 1.2 million reads per group) (Table S2).

The overall read mapping rate to the *de novo* transcriptome assembly ranged between 83 % and 86 % across samples (Table S3). We found a total of 390 complete orthologues, out of which 73 % were complete and single copy. In total, 26,638 transcripts were successfully annotated. A summary of the main GO terms in the annotated transcriptome is shown in Table S3.

3.1. Genetic structure

We found no evidence of genetic differentiation among populations of the copper moss *S. cataractae*. The AMOVA test showed a very low percent of genetic variation among populations (0.01 %; $\varphi = 0.0001$), and the randomization test performed on the output of the AMOVA was not significant (p-value = 0.462). Similarly, the permutation test carried out to assess the significance of the G-statistic was not significant (G-stat = 83712.2; p = 0.839). The lack of genetic differences among populations is shown in Fig. S1.

3.2. Epigenetic changes in response to Cd and Cu

Overall, DNA methylation in *S. cataractae* was very low (Table 1). For the complete SMP matrix (n = 43,365 SMPs) mean cytosine methylation per group averaged 3.3 % $\pm$ 0.06 in all contexts considered together, and 0.69 % $\pm$ 0.05 in CG, 12 % $\pm$ 0.05 in CHG, and 0.71 % $\pm$ 0.07 in CHH. Most of the cytosines in the CG, CHG, and CHH contexts were unmethylated, i.e. methylation level $\leq$ 5 % in $\geq$ 95 % of the samples (92.6 % in CG, 91.2 % in CHH and 81.9 % in CHG); 1.9 % of the cytosines in the CHG context were fully methylated, i.e. methylation level $\geq$ 95 % in $\geq$ 95 % of the samples (Fig. S2A). The standard deviation of DNA methylation averaged 16.0 % $\pm$ 0.07 in all contexts together, and 3.1 % $\pm$ 0.39 in CG, 31.5 % $\pm$ 0.05 in CHG, and 2.8 % $\pm$ 0.39 in CHH (Table 1). For the complete and polymorphic SMP matrix (n = 3769 SMPs), mean cytosine methylation per group averaged 10.8 % $\pm$ 0.25 in all contexts, and 2.8 % $\pm$ 0.26 in CG, 34.3 % $\pm$ 0.23 in CHG, and 2.4 % $\pm$ 0.32 in CHH (Fig. S2B). The standard deviation of DNA methylation averaged 27.5 % $\pm$ 0.15 in all contexts, and 7.2 % $\pm$ 0.88 in CG, 45.3 % $\pm$ 0.18 in CHG, and 5.3 % $\pm$ 0.86 in CHH (Table 1).

DNA methylation levels differed among genomic features with repeats generally showing higher methylation levels than genes and transposons; for example, mean methylation across samples in repeats was 0.9 %, 12.6 %, and 1 % in the CG, CHG, and CHH contexts respectively compared to the ~0.5 %, 10.2 %, and 0.6 % in the CG, CHG, and CHH contexts found for genes and transposons respectively (Fig. S3).

We found there was no significant effect of population, treatment, or their interaction on genome wide DNA methylation in *S. cataractae* when we used only the epigenetic distance matrix in dbRDA (Table S4). When we used the distance matrices of both methylation level and methylation variance between samples, the model was significant for both common garden experiments, and explained 61 % and 56 % of the variation of the epigenetic distances in the Cd vs. C and the Cu vs. C comparison respectively (Table 2; results for each separate sequence context were similar and are shown in Table S4). The effect of both predictors and their interaction was significant in both experiments: treatment explained ~9 % and 7 % of the variation of the epigenetic distances in the Cd vs. C and Cu vs. C comparisons respectively; population explained ~21 % of the variation in both experiments; and the interaction explained 33 % and 29 % of the variation in the Cd vs. C and Cu vs. C comparisons respectively (Table 2).

Both metal treatments induced more DNA methylation variation among samples of Sc2 (one of the most metal tolerant populations). This effect was weaker, yet noticeable on Sc1 and Sc2 in response to Cu, and on Sc4 in response to Cd (Fig. 1A1, A2). The first two constrained axes of the dbRDA explained ~35 % and ~29 % of the variation in epigenetic distances in the Cd vs. C and the Cu vs. C comparison respectively. Most of the variation in the first axis (RDA1) was driven by the differentiation of treated samples from Sc2 in both common garden experiments, whereas most of the variation in the second axis (RDA2) was driven by the differentiation of control samples from Sc3 and Sc4 in the two common garden experiments (Fig.1A1, A2).

We found between 25 and 78 differentially methylated positions (DMPs) between Cd-treated and control (Fig. 1B1) and Cu-treated and control plants (Fig. 1B2) across populations (between 0.66 % and 2.1 %

Table 1
Average DNA methylation (Mean) and standard deviation of DNA methylation (Std. Dev.) per group (i.e. each unique population – Pop. - and treatment – Treat. - combination) for each separate sequence context (CG, CHG, CHH), and across all contexts (all) in samples of the copper moss *Scopelophila cataractae* obtained with the complete single methylation polymorphism matrix (All SMPs; n = 43,365 SMPs), and the ccomplete and polymorphic matrix (Polym. SMPs; n = 3769 SMPs).

Pop	Treat	Dataset	CG		CHG		CHH		all	
			Mean	Std. Dev.	Mean	Std. Dev.	Mean	Std. Dev.	Mean	Std. Dev.
Sc1	C	All SMPs	0.63	2.33	11.98	31.49	0.66	2.34	3.25	15.95
	Cd		0.64	3.36	12.06	31.64	0.67	3.17	3.28	16.15
	Cu		0.74	3.04	12.07	31.51	0.81	2.83	3.38	16.03
	C	Polim. SMPs	2.38	4.98	34.39	45.38	2.29	4.22	10.67	27.37
	Cd		2.75	7.70	34.61	45.66	2.29	5.94	10.81	27.81
	Cu		2.96	7.16	34.45	45.27	2.85	5.00	11.10	27.38
Sc2	C	All SMPs	0.70	3.64	12.09	31.64	0.69	3.36	3.31	16.19
	Cd		0.76	3.27	12.15	31.55	0.80	2.99	3.40	16.08
	Cu		0.73	2.86	12.09	31.52	0.71	2.54	3.33	16.01
	C	Polim. SMPs	2.87	8.10	34.89	45.48	2.51	6.30	11.02	27.82
	Cd		3.06	7.70	35.00	45.23	2.60	5.18	11.14	27.57
	Cu		3.21	7.05	34.43	45.49	2.33	4.81	10.88	27.51
Sc3	C	All SMPs	0.74	3.69	12.05	31.51	0.78	3.53	3.36	16.14
	Cd		0.66	3.04	12.04	31.52	0.72	3.03	3.30	16.06
	Cu		0.66	2.64	12.05	31.53	0.74	2.52	3.32	16.00
	C	Polim. SMPs	3.17	8.53	34.61	44.98	2.75	6.74	11.14	27.57
	Cd		2.72	7.50	34.42	45.44	2.60	5.89	10.92	27.61
	Cu		2.89	7.08	34.73	45.25	2.77	5.43	11.12	27.48
Sc4	C	All SMPs	0.64	3.01	11.98	31.52	0.59	2.44	3.22	16.01
	Cd		0.75	2.80	12.11	31.50	0.72	2.41	3.34	15.99
	Cu		0.61	3.06	12.00	31.58	0.62	2.94	3.23	16.08
	C	Polim. SMPs	2.44	7.34	34.24	45.23	1.71	4.05	10.34	27.46
	Cd		2.88	6.79	34.68	45.27	2.22	4.08	10.81	27.44
	Cu		2.62	6.81	34.33	45.59	2.08	5.20	10.59	27.63

Table 2
Results of the distance-based redundancy analysis (dbRDA) carried out to test the effect of population, treatment, and their interaction on genome wide DNA methylation for each of the common garden experiments (Overall model). The results of the permutation test (n = 9999) for the significance of each of the predictors are also shown (Predictors). d_{st}: pairwise distance matrix calculated with the methylation level and variance of each cytosine in each sample. CG-Cd: common garden comparing control and Cd-treated plants; CG-Cu: common garden comparing control and Cu-treated plants; Df: degrees of freedom; adj. R^2: adjusted R^2.

Experiment	Response	Model	Predictor	Df	Variance	F	Pr (>F)	adj. R^2
CG-Cd	d_{st}	Overall model	Model	7	11405	5.08	0.0001	61.3
			Residual	11	3531			
		Predictors	Population	3	4916	5.11	0.0001	21.6
			Treatment	1	1685	5.25	0.0001	8.8
			Pop.:Treat.	3	4803	4.99	0.0001	33.1
			Residual	11	3531			
CG-Cu	d_{st}	Overall model	Model	7	10859	4.48	0.0001	56.2
			Residual	12	4152			
		Predictors	Population	3	4881	4.70	0.0001	21.3
			Treatment	1	1456	4.21	0.0001	7.0
			Pop.:Treat.	3	4522	4.36	0.0001	29.4
			Residual	12	4152			

of the polymorphic cytosines; Fig. S4). All populations showed more DMPs within the CHH context (17 %, 26 %, and 57 % of all DMPs in CG, CHG, and CHH contexts respectively; Table S5) but the proportion of DMPs per context did not differ from the proportion of cytosines interrogated per context. Sc3 showed the highest number of DMPs in both treatments (Figs. 1B1, 1B2, S4). Cadmium induced more DMPs than Cu (except in Sc4; Figs. 1B1, 1B2, S4). We found more DMPs with a negative methylation change, i.e. hypomethylation, in Sc2 in response to Cd and Cu, and in Sc3 in response to Cu; Sc1 and Sc4 showed more DMPs with a positive methylation change, i.e. hypermethylation, in response to Cd and Cu respectively. Most DMPs were unique for each population except four: two shared between Sc1 and Sc2 and one shared between Sc1 and Sc4 in the Cd vs. C comparison; one shared between Sc3 and Sc4 in the Cu vs. C comparison (Fig. S5A, S5B). The two metals, however, induced a considerable number of common DMPs within each population, most of which were hypomethylated: 29 %, 49 %, 41 %, and 12 % of the DMPs were common to both treatments in Sc1 to Sc4 respectively (Fig. S5C, underlined DMPs in Table S5).

3.3. Effect of Cu on gene expression

Copper exposure significantly affected transcript expression profiles in plants from the two studied populations. The effect of Cu was greater in the most tolerant population (Sc3) as shown by: (i) the greatest separation between control and Cu-treated samples of Sc3 in the multidimensional scaling plot (Fig. 1C1); (ii) the greater number of DETs in Sc3 than in Sc4, i.e. 1710 DETs in Sc3 - 7.4 % of the total - and 259 DETs in Sc4 - 1.1 % of the total; and (iii) the greater expression changes shown by DETs in Sc3 compared to the same DETs in Sc4 (Fig. 1C2; Fig. S6). The majority of the DETs found in each population were down-regulated in response to treatment, i.e. 99 % and 95 % in Sc3 and Sc4 respectively (Table S6), indicating that these transcripts were constitutively expressed in control plants, and their expression was significantly repressed in response to Cu. The direction of the expression change, i.e. up- or downregulation, of the 220 DETs that were common to both populations was the same; the intensity of the change, however, was ≥ 2 times higher in Sc3 for 62 % of the common DETs (on average, FC in this fraction of DETs was 9x higher in Sc3 compared to Sc4); the opposite

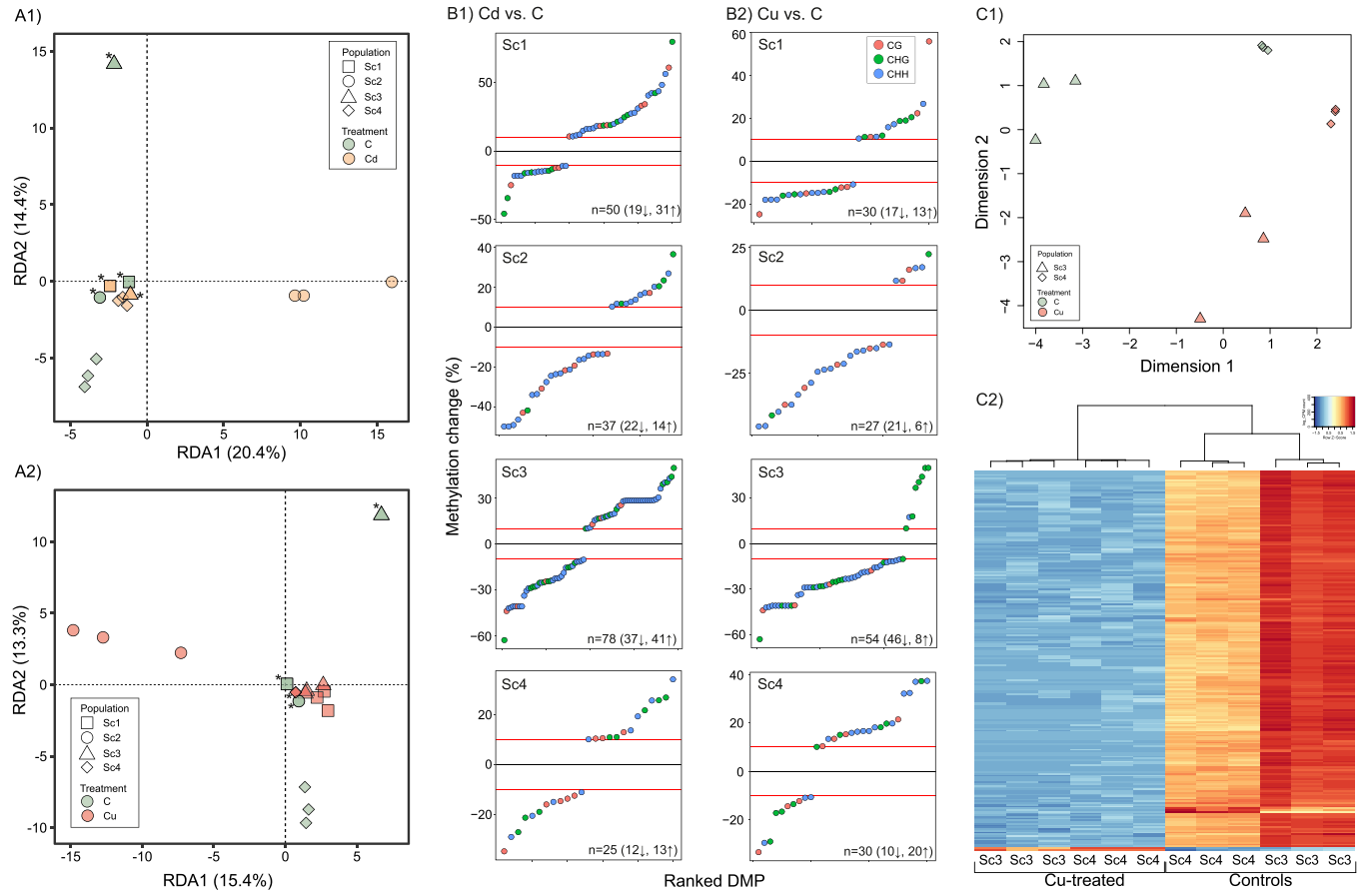

Fig. 1. Left panel: ordination plots of the distance-based redundancy analysis (dbRDA) on the epigenetic distances between cadmium-treated and control plants (Cd vs. C; A1), and between copper-treated and control plants (Cu vs. C; A2) from four populations of the copper moss *Scopelophila cataractae* (n = 2–3 replicates per population and treatment). RDA1: first constrained ordination axis explaining 20.6 (A1) and 15.2 (A2) of the total variance of the data; RDA2: second constrained ordination axis explaining 14.3 (A1) and 13.3 (A2) of the total variance of the data. Asterisks mark overlapping observations from the same group. Central panel: difference in the methylation level (i.e. methylation change) of differentially methylated cytosine positions (DMPs; fdr < 0.05) between cadmium-treated and control plants (Cd vs. C; B1), and between copper-treated and control plants (Cu vs. C; B2) from four populations of the copper moss *Scopelophila cataractae* (Sc1 to Sc4); values at the bottom of each graph indicate the number of DMPs for each contrast (↑: up-methylated; ↓: down-methylated); red lines delimit the area in which absolute methylation differences are lower than 10. Right panel: multidimensional scaling (MDS) plot of the gene expression profiles in control and Cu-treated samples from two populations of the copper moss *Scopelophila cataractae* (Sc3 and Sc4; C1). Heatmap of the normalized expression levels (i.e. Row z-scores) of the differentially expressed transcripts in response to Cu shared between Sc3 and Sc4 (C2).

was true in only 9 % of the common DETs (with an average FC in this fraction of DETs 3.4x higher in Sc4 than Sc3) (Fig. 1C2, S6, Table S6).

In total, 74 % and 76 % of the DETs were annotated in Sc3 and Sc4 respectively (Table S6). The results of the Fisher's exact test showed 117 over-represented and 13 under-represented GO terms in Sc3, and 11 over-represented GO terms in Sc4 in the lists of DETs compared to the full list of transcripts (Table S7). The most over-represented molecular functions in Sc3 included terms related to RNA metabolism and ribosomal structure (RNA binding, GO:0003723; structural constituent of ribosome, GO:0003735), protein molecular interactions (protein-containing complex binding GO:0044877; protein homodimerization activity; GO:0042803; protein N-terminus binding, GO:0047485), glycosidic bond hydrolysis (hydrolase activity, hydrolyzing O-glycosyl compounds, GO:0004553), protein hydrolysis and its regulation (exopeptidase activity, GO:0008238; serine-type endopeptidase activity, GO:0004252; endopeptidase inhibitor activity, GO:0004866), redox activity (oxidoreductase activity, GO:0016715), and Ca signaling/regulation (Ca ion binding, GO:0005509). These functions were only represented within the down-regulated DETs list (except Ca ion binding, also present within the up-regulated DETs; Table S7). Over-represented molecular functions in Sc4 consisted of protein hydrolysis (cysteine-type endopeptidase activity, GO:0004197; serine-type endopeptidase activity, GO:0004252), chitin binding (GO:0008061), and structural molecule activity (GO:0005198), all of which were only represented in the down-regulated DETs list (Table S5). The GO terms related to biological process, molecular function, and cellular component associated to all DETs of each population are shown in Fig. S7.

We classified down-regulated DETs from Sc3 and Sc4 into 13 different functional groups according to their annotation descriptions (Table S8; Fig. 2C,D) which included transcripts related to: i) protein and ribosome biosynthesis, including structural constituents of ribosomal subunits as well as transcripts involved in protein transcription, translation and elongation; ii) protein degradation and/or turnover, including many proteases, transcripts involved in protein ubiquitination, and structural components and regulators of the proteasome; iii) transcripts with reduction-oxidation (redox) activity, including components of the reactive oxygen species (ROS) scavenging systems (e.g. glutathione S-transferase, ascorbate peroxidase, catalase); iv) protein repair and proper protein folding activity, mostly comprised by protein chaperones; v) Ca homeostasis and signal transduction including Ca-transporting ATPases, Ca calmodulin-dependent kinases, and calmodulin; vi) energy metabolism including enzymes involved in glycolysis, pentose-phosphate, and tricarboxylic acid cycle pathways; vii) transmembrane transport like V-type proton ATPases, ABC transporters, or zinc finger proteins; viii) RNA metabolism, including RNA helicases, mRNA splicing factors, and rRNA processing factors. The remaining

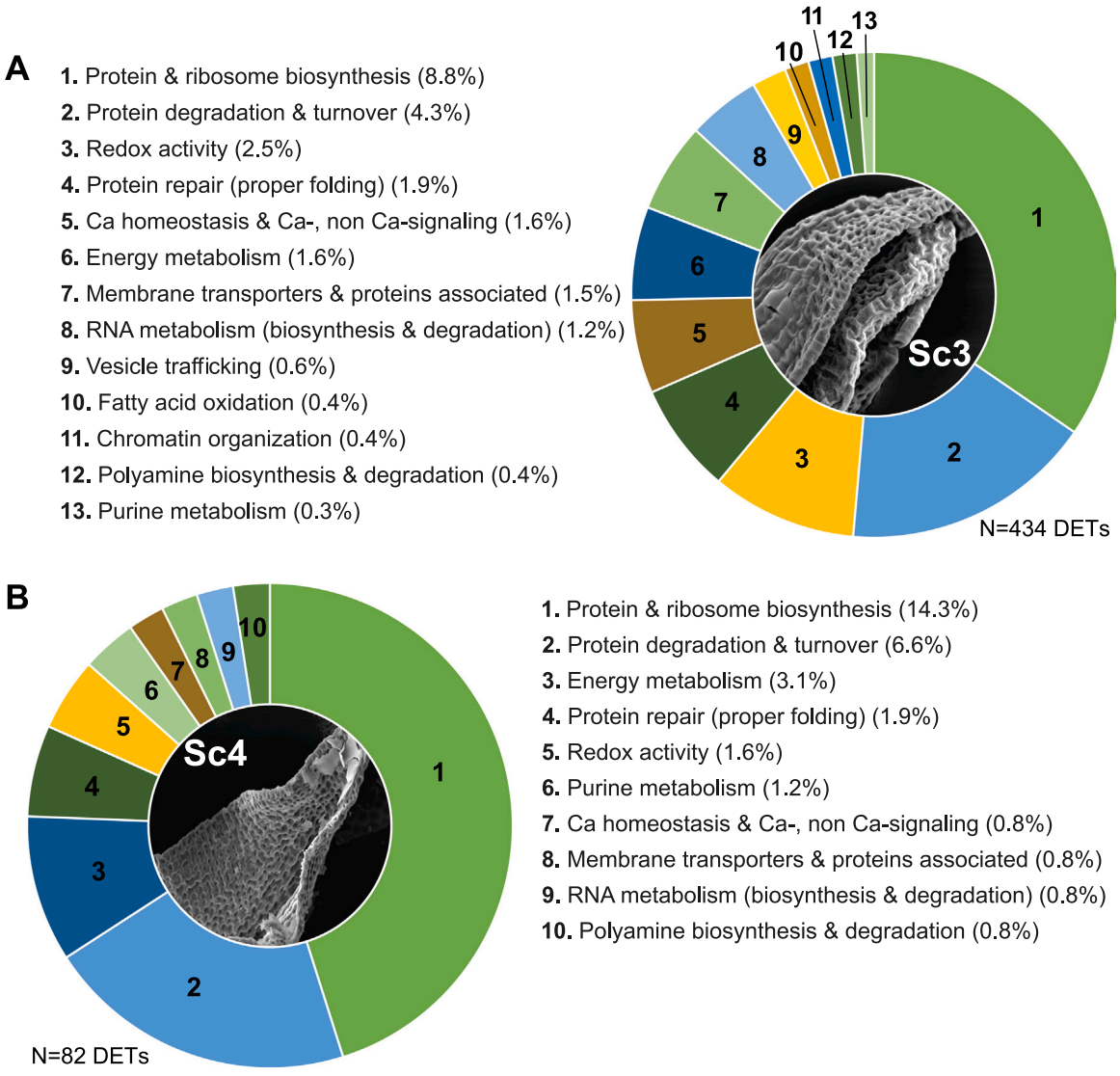

Fig. 2. Circular plots of the functional categories created by grouping downregulated transcripts of Sc3 (A) and Sc4 (B) in response to Cu according to their annotation descriptions. The percent of transcripts within each group with respect to the total number of DETs is shown between parentheses. N: total number of DETs included in this classification for each population.

groups included transcripts related to vesicle trafficking, fatty acid oxidation, chromatin organization, polyamine biosynthesis and degradation, and purine metabolism. For Sc4, all transcripts except those involved in vesicle trafficking, fatty acid oxidation, and chromatin organization, were represented within the down-regulated DETs list, although the number of transcripts within each group was significantly lower (Fig. 2D; Table S8).

Up-regulated transcripts in Sc3 included enzymes involved in the regulation of the redox state of the cells (probable 2-oxoglutarate-dependent dioxygenase ANS, L-ascorbate oxidase-like, cytokinin hydroxylase, and peroxidase P7-like), and transcripts were involved in cellular signaling processes (EG45-like domain containing protein) and lipid hydrolysis (GDSL esterase/lipase). Three transcripts were up-regulated both in Sc3 and Sc4: allene oxide cyclase, an enzyme catalyzing the most important step in the jasmonic acid (JA) biosynthetic pathway; CML25, a member of the calmodulin-like protein group; and L-ascorbate oxidase-like protein, involved in the regulation of the redox status of the cells. Uniquely up-regulated DETs in Sc4 included the metal homeostasis factor ATX1-like, a copper chaperone that delivers Cu to heavy metal P-type ATPases, two probable copper-transporting ATPases (HMA5), involved in copper transport across membranes, two dehydrogenases with oxidoreductase activity (alcohol dehydrogenase 1-like; and aldehyde dehydrogenase family 2 member B7, mitochondrial-like), and one primary amine oxidase-like, involved in polyamine degradation (descriptions as well as expression changes of all DETs are present in Table S6).

Finally, we found 100 DETs between control plants from Sc3 and Sc4; 68 DETs were significantly upregulated and 32 were downregulated in plants from Sc3 compared to those from Sc4. Annotated upregulated DETs showed a greater expression of components of the protein biosynthesis and degradation machinery and signal transduction, which were downregulated in response to Cu in both populations. Annotated downregulated DETs, on the other hand, were related to the energy metabolism and vacuole transport, among others (Table S6).

3.4. Relationship between DNA methylation and expression changes

A total of 12,631 contigs from the *de novo* genome mapped to 8623 transcripts but none of the DMPs mapped to any of the DETs. Yet, multiple contigs with DMPs mapped to transcripts that were annotated; descriptions of these sequences matched some of the main processes down-regulated during Cu-exposure such as protein degradation/

turnover, chromatin organization, membrane transporters or signal transduction (Table S4).

4. Discussion

In this work, we used epiGBS and RNAseq to study the drivers of intraspecific variation for heavy metal tolerance in the copper moss *S. cataractae*, and to provide new insights into the molecular mechanisms used by bryophytes to deal with heavy metal toxicity. Our results showed that (i) genetic differentiation did not explain phenotypic differences in Cd and Cu tolerance in *S. cataractae*; (ii) heavy metal exposure induced some DNA methylation changes. These, however, were inconsistent within treatment groups leading to an increase in methylation variation in Cd- and/or Cu-treated plants in plants from the most tolerant populations; (iii) single cytosine methylation changes (SMPs) tended to hypomethylation in the most tolerant populations and to hypermethylation in the least tolerant ones; (iv) plants from both the more and the less tolerant populations constitutively expressed multiple genes involved in heavy metal tolerance in the absence of Cu in the laboratory. The most tolerant plants, however, expressed more genes involved in the alleviation of heavy metal stress under control conditions, whereas the less tolerant invested more in growth; and v) upon acute Cu stress, both populations inhibited the expression of these protective genes to nearly equivalent levels. The magnitude of this inhibition was greater in the more tolerant population. Altogether, these results suggest that chronic exposure to different levels of heavy metals in the field is associated with non-genetically-based intraspecific differentiation for heavy metal tolerance in *S. cataractae*. At the molecular level, this phenotypic differentiation was reflected in a greater constitutive investment in protective mechanisms (e.g. ROS scavenging enzymes, heavy metal transporters, protein chaperones) in the most tolerant population, but maintaining an equivalent response into an energy conservative state when facing an acute Cu stress event in the laboratory.

Scopelophila cataractae is called “copper moss” due to its high affinity for heavy metals, especially Cu. In fact, its worldwide geographical distribution mostly matches that of Cu-enriched substrates (Shaw, 1993a; Shaw, 1995; Shaw, 1987), and its growth has been consistently stimulated by Cu in the laboratory (Nomura and Hasezawa, 2011; Shaw, 1993b). Yet, previous studies have shown that this metal compromises the species’ growth upon exposure to high concentrations of bioavailable Cu (Boquete et al., 2021; Nomura and Hasezawa, 2011), and that this acute Cu stress can uncover novel intraspecific variation in Cu tolerance (Boquete et al., 2021a). In our previous study, we reported phenotypic differentiation for Cd and Cu tolerance among plants from the same populations studied here: growth of plants from populations that originated from more contaminated microhabitats was increased (Sc2) or unaffected (Sc3) in metal-treated compared to control plants, whereas growth of plants from populations that originated from less contaminated microhabitats (Sc3, Sc4) was reduced (Boquete et al., 2021). These differences were observed after clonally propagating all plants in control conditions several times for a year, which should have eliminated any potential carryover environmental effects from the field. Taken together, these findings supported a role of natural selection in generating locally adapted genotypes among the four populations. Nonetheless, our current results showed no evidence of genetic differentiation among the populations studied, at least in the portion of the genome interrogated with the epiGBS technique. The lack of genetic differentiation could be explained by the movement of gametophore fragments and asexual propagules down the slope of the field site (~500 m long). Thus, our analysis suggested that this phenotypic differentiation could have arisen through mechanisms other than DNA sequence variation.

In the past few decades, epigenetic variation has emerged as a potentially important source of phenotypic variation and differentiation in plants (Herrera and Bazaga, 2013; Róis, 2013; Alonso et al., 2014; Medrano et al., 2014; Platt et al., 2015; Richards and Pigliucci, 2020; Puy, 2021). Thus, we assessed whether DNA methylation contributed to the differences in tolerance observed in our common garden experiments. We did not find evidence for epigenetic differentiation among populations when we compared mean methylation levels across all cytosines, and the effect of Cd and Cu exposure on individual cytosine methylation levels was rather limited compared to response to other stresses in other plants (e.g. (Yadav, 2020)). We propose three possible causes for this limited response. First of all, environmental stress can increase inter-individual methylation variation in plants (Verhoeven et al., 2010). This type of inconsistency would limit our capacity to find clear directional changes between experimental groups. In this study, we found a significant increase in DNA methylation variation in plants from Sc2 in response to both metal treatments, and a slight increase in variation in plants from Sc1 and Sc3 in response to Cu, and from Sc4 in response to Cd. Although this effect needs to be further validated with a greater number of replicate samples per treatment group, these results support a potential population-specific epigenetic response to heavy metal exposure. Even though it has not been experimentally proven, such stress-induced inter-individual epigenetic variation could contribute to increased population-level phenotypic variation and help plant populations to deal with environmental stress (Boquete et al., 2021b).

On the other hand, the limited epigenetic response found here could also be due, in part, to fundamental differences between the epigenomic landscape of bryophytes and angiosperms, combined with the technical characteristics of the epiGBS technique. Overall, bryophyte genomes are much less methylated than angiosperm genomes (Lang, 2018; Diop, 2020) (but see (Schmid, 2018) for differences among stages of the bryophyte life cycle), and cytosine methylation tends to be segregated away from genic regions (Zemach et al., 2010). For example, in contrast to flowering plants, gene body methylation (gbM) is absent in most genes of the model moss *P. patens* (Lang, 2018) and the model liverwort *Marchantia polymorpha* (Diop, 2020) (but see (Schmid, 2018)). The epiGBS technique interrogates a biased subset of the genome, as the restriction enzyme that we used, *Pst*I, preferentially targets coding regions (van Gurp, 2016). Together with the low gbM found for other bryophytes, this would explain the very low DNA methylation levels found here, and the limited response to heavy metal exposure within the interrogated genomic regions. Further, our epiGBS fragments did not overlap with our DETs so we had no information about the methylation status of those specific transcripts (as reported in (Alvarez, 2020; Robertson, 2020). Finally, it is also possible that epigenetic mechanisms other than DNA methylation, or even point mutations located in genomic regions other than that interrogated here, could determine the phenotypic differences observed here. For example, several proteins involved in chromatin reorganization were only differentially expressed in the more tolerant population. This included the histone modifying enzyme histone deacetylase 6 and its associated WD-40 repeat-containing protein MSI1 purported to be involved in epigenetic regulation of plant stress tolerance (Patanun, 2017; Mehdi, 2016), the histone chaperone peptidyl-prolyl cis-trans isomerase FKBP53, and the SWI/SNF-related matrix-associated actin-dependent regulator of chromatin subfamily A member 5. These findings suggest a potential role of histone modifications in heavy metal stress tolerance in *S. cataractae*.

Some authors have pointed out that changes in DNA methylation in response to heavy metal stress could be due to a side effect of metal-induced ROS production (Aina, 2004). However, some of the patterns observed here indicate otherwise. First, exposure to Cd induced more methylation changes despite the lack of a significant increase in oxidative damage in any of the populations studied (Fig. 3 H in (Boquete et al., 2021a)). Second, the effect of Cd and Cu on DNA methylation was population-specific, with more methylation variation induced in one of the most tolerant moss populations (Sc2). Third, more cytosines were hypo- than hypermethylated in plants from the most tolerant populations (Sc2, Sc3), while we observed the opposite trend in the less

tolerant ones (Sc1, Sc4). Finally, when compared within each population, both metals induced numerous common DMPs. Together, these findings suggest that the DNA methylation changes observed here were not random, as expected if generated through metal-induced ROS production, but likely dependent on the previous stress experience of the plants.

The set of DETs found in this study provided valuable information about the potential adaptive mechanisms developed to deal with chronic Cu exposure in natural conditions for *S. cataractae*. For example, 16.2 % and 23.6 % of all DETs in Sc3 and Sc4 respectively, were involved in cellular protein homeostasis including protein and RNA biosynthesis/degradation, and protein repair. Heavy metals can disrupt protein folding and cause aggregation (Shahid, 2014; Hasan, 2017; Lemire et al., 2013; Tamás et al., 2014). Aggregation and accumulation of unfolded proteins triggers the unfolded protein response (UPR) pathway, which enhances protein folding and degradation, and reduces protein production under stress conditions (Hasan, 2017). Multiple components of the UPR pathway were constitutively expressed in *S. cataractae*, including components of the calnexin/calreticulin complex as well as protein chaperones involved in protein folding, the Ubiquitin-26S proteasome proteolytic system, and multiple translation and elongation initiation factors involved in protein synthesis.

Similarly, a considerable number of constitutively expressed transcripts were involved in direct or indirect ROS detoxification (e.g. glutathione S-transferases, L-ascorbate peroxidases, superoxide dismutases), cellular signaling, trafficking and metal transport (e.g. calmodulins, clathrins, ras-related proteins, V-type proton ATPases, zinc finger proteins, ABC transporters), fatty acid oxidation enzymes related to the jasmonic acid biosynthetic pathway (e.g. peroxisomal acyl-CoA oxidase, 3-ketoacyl-CoA thiolase), and purine metabolism (adenosine kinases, inosine-5′-monophosphate dehydrogenase). Polyamine metabolism, including enzymes like ornithine decarboxylase, S-adenosylmethionine synthase, and spermidine synthase, was also associated with the response to Cu in *S. cataractae*. These organic compounds have been shown to increase heavy metal tolerance in plants through ROS detoxification (Choudhary et al., 2012; Hussain et al., 2019; Nahar et al., 2017) and decreased metal accumulation (Choudhary et al., 2012; Wang et al., 2007). The functioning of all these stress alleviation mechanisms is energy and carbon consuming, which explains the increased constitutive expression of enzymes involved in energy production like the glycolysis, penthose-phosphate, and tricarboxylic acid pathways (Sarry, 2006).

Finally, we cannot discard that some of the changes in transcript abundance observed here were due to differences in RNA turnover rates (i.e. post-translational regulation within the RNA metabolism; Fig. 2C, D) under heavy metal exposure rather than on and off switches in gene expression (i.e. translational regulation) as has been shown before for other plants under osmotic and salt stress (Kawa and Testerink, 2017).

In this study, we found evidence of potentially non-genetically-based phenotypic differentiation for heavy metal tolerance in bryophytes. Our results indicated that chronic exposure to high concentrations of metals in natural conditions led to constitutive overexpression of genes that contribute to heavy metal stress tolerance in several ways (e.g. regulation of cellular protein homeostasis, ROS detoxification, metal transport). Importantly, plants that had grown under higher stress conditions in the field were more tolerant to acute Cu stress events like that used in our experiments, possibly due to their greater capacity to decrease production of energetically expensive products as a strategy to reduce energy consumption in a situation in which the ability of these mechanisms to provide protection against the stress would be overwhelmed. Based on the higher epigenetic response of the most tolerant populations (greater changes in DNA methylation and constitutive expression of chromatin remodeling proteins) we propose that their increased capacity to regulate the expression of heavy metal stress-related genes could have an epigenetic basis that we could not detect with our approach. This work thus serves as a proof of concept for future studies which should focus on the targeted evaluation of the regulatory mechanisms presented here, and evaluate their relative importance in heavy metal stress tolerance in bryophytes.

Funding information

This research has received funding from the European Union's Horizon 2020 and is currently supported by the Maria Zambrano program by the Spanish Ministry of Science, Innovation and Universities. research and innovation programme under the Marie Skłodowska-Curie grant agreement No 704141-BryOmics. Dr. M. Teresa Boquete has been supported during the development of this project by the Juan de la Cierva-Incorporación program from the Spanish Ministry of Science, Innovation and Universities (IJC2018-035018).

CRediT authorship contribution statement

MTB, CLR, and CA conceived and designed the experiments; MTB, SC, and NCAM performed the wet lab work; MTB and MWS performed the data analyses; MTB wrote first draft of the manuscript; MTB, CA, CLR, SFM, SC, MWS, and NCAMW critically reviewed and edited the manuscript.

Declaration of Competing Interest

The authors declare that they have no known competing financial interests or personal relationships that could have appeared to influence the work reported in this chapter.

Data Availability

The pipeline scripts used for this study are available at: https://github.com/thomasvangurp/epiGBS, with a bug-fix modification (https://github.com/MWSchmid/epiGBS_Nov_2017_fixed). The raw sequence data files for epiGBS (Illumina paired end reads), and for RNAseq (individual samples' Illumina paired end reads after quality trimming) have been submitted to the Sequence Read Archive (SRA) of NCBI under project number PRJNA790924 (https://www.ncbi.nlm.nih.gov/bioproject/PRJNA790924). The barcodes (barcodes.tsv) required to process the raw epiGBS sequencing data available on SRA, the reference contigs (de_novo_contigs.fasta.gz), the annotation of the reference contigs (mergedAnnot.csv.gz), the SNPs (snps.vcf.gz), the methylation data (methylation.txt.gz), and the de novo transcriptome assembly (de_novo_transcriptome.fasta.gz) are available on zenodo (https://doi.org/10.5281/zenodo.6695117).

Acknowledgments

We thank Dr. Carlos M. Herrera for his advice throughout the development of the project; we also thank Dr. Jonathan A. Shaw and Dr. Blanka Aguero for their help with field sample localization and collection, Luiza Silva Simoes and Olivia Santiago for help during laboratory work at USF, and Dr. Mariano Alvarez, Dr. Marta Robertson, Dr. Sabrina McNew, Dr. Jeannie Mounguer, and Sandra Voors for continuous discussions and feedback about the epiGBS data analyses. This research has received funding from the European Union's Horizon 2020 research and innovation programme under the Marie Skłodowska-Curie grant agreement No 704141-BryOmics. Dr. M. Teresa Boquete has been supported during the development of this project by the Juan de la Cierva-Incorporación program from the Spanish Ministry of Science, Innovation and Universities (IJC2018-035018) and is currently supported by the Maria Zambrano program from the Spanish Ministry of Science, Innovation and Universities.

Appendix A. Supporting information

Supplementary data associated with this article can be found in the online version at doi:10.1016/j.envexpbot.2022.104970.

References

Agar, G., et al., 2014. Effects of lead sulfate on genetic and epigenetic changes, and endogenous hormone levels in corn (Zea mays L.). Pol. J. Environ. Stud. 23, 1925–1932.

Aina, R., et al., 2004. Specific hypomethylation of DNA is induced by heavy metals in white clover and industrial hemp. Physiol. Plant. 121, 472–480.

Ali, H., Khan, E., Ilahi, I., 2019. Environmental chemistry and ecotoxicology of hazardous heavy metals: environmental persistence, toxicity, and bioaccumulation. J. Chem. 2019, e6730305.

Alonso, C., Pérez, R., Bazaga, P., Medrano, M., Herrera, C.M., 2014. Individual variation in size and fecundity is correlated with differences in global DNA cytosine methylation in the perennial herb Helleborus foetidus (Ranunculaceae). Am. J. Bot. 101, 1309–1313.

Al-Shahrour, F., Díaz-Uriarte, R., Dopazo, J., 2004. FatiGO: a web tool for finding significant associations of Gene Ontology terms with groups of genes. Bioinformatics 20, 578–580.

Alvarez, M. et al. Reduced representation characterization of genetic and epigenetic differentiation to oil pollution in the foundation plant Spartina alterniflora. 426569 ⟨https://www.biorxiv.org/content/10.1101/426569v3⟩ (2020) doi:10.1101/426569.

Antreich, S., Sassmann, S., Lang, I., 2016. Limited accumulation of copper in heavy metal adapted mosses. Plant Physiol. Biochem. 101, 141–148.

Assche, F.V., Clijsters, H., 1990. Effects of metals on enzyme activity in plants. Plant, Cell Environ. 13, 195–206.

Bartee, L., Shriner, W. & Creech, C. Eukaryotic epigenetic regulation. (2017).

Becher, M., Talke, I.N., Krall, L., Krämer, U., 2004. Cross-species microarray transcript profiling reveals high constitutive expression of metal homeostasis genes in shoots of the zinc hyperaccumulator Arabidopsis halleri. Plant J. 37, 251–268.

Bednarek, P.T., Orłowska, R., Niedziela, A., 2017. A relative quantitative methylation-sensitive amplified polymorphism (MSAP) method for the analysis of abiotic stress. BMC Plant Biol. 17, 79.

Bellini, E., et al., 2020. The moss leptodictyum riparium counteracts severe cadmium stress by activation of glutathione transferase and phytochelatin synthase, but slightly by phytochelatins. Int. J. Mol. Sci. 21, 1583.

Bolger, A.M., Lohse, M., Usadel, B., 2014. Trimmomatic: a flexible trimmer for Illumina sequence data. Bioinformatics 30, 2114–2120.

Boominathan, R., Doran, P.M., 2002. Ni-induced oxidative stress in roots of the Ni hyperaccumulator, Alyssum bertolonii. N. Phytol. 156, 205–215.

Boquete, M.T., Lang, I., Weidinger, M., Richards, C.L., Alonso, C., 2021a. Patterns and mechanisms of heavy metal accumulation and tolerance in two terrestrial moss species with contrasting habitat specialization. Environ. Exp. Bot. 182, 104336 https://doi.org/10.1016/j.envexpbot.2020.104336.

Boquete, M.T., Muyle, A., Alonso, C., 2021b. Plant epigenetics: phenotypic and functional diversity beyond the DNA sequence. Am. J. Bot. 108, 553–558. https://doi.org/10.1002/ajb2.1645.

Brown, D.H., Wells, J.M., 1990. Physiological effects of heavy metals on the moss rhytidiadelphus squarrosus. Ann. Bot. 66, 641–647.

Buchfink, B., Xie, C., Huson, D.H., 2015. Fast and sensitive protein alignment using DIAMOND. Nat. Methods 12, 59–60.

Choudhary, S.P., Kanwar, M., Bhardwaj, R., Yu, J.-Q., Tran, L.-S.P., 2012. Chromium stress mitigation by polyamine-brassinosteroid application involves phytohormonal and physiological strategies in Raphanus sativus L. PLOS ONE 7, e33210.

Cicatelli, A., et al., 2014. Epigenetic control of heavy metal stress response in mycorrhizal versus non-mycorrhizal poplar plants. Environ. Sci. Pollut. Res. 21, 1723–1737.

Conesa, A., et al., 2005. Blast2GO: a universal tool for annotation, visualization and analysis in functional genomics research. Bioinformatics 21, 3674–3676.

Cong, W., et al., 2019. Transgenerational memory of gene expression changes induced by heavy metal stress in rice (Oryza sativa L.). BMC Plant Biol. 19, 282.

R. Core Team . R: A language and environment for statistical computing. R Foundation for Statistical Computing, Vienna, Austria. (2018).

Devi, S.R., Prasad, M.N.V., 1999. Membrane Lipid Alterations in Heavy Metal Exposed Plants. In: Prasad, M.N.V., Hagemeyer, J. (Eds.), in Heavy Metal Stress in Plants: From Molecules to Ecosystems. Springer, pp. 99–116. https://doi.org/10.1007/978-3-662-07745-0_5.

Ding, Y., Chen, Z., Zhu, C., 2011. Microarray-based analysis of cadmium-responsive microRNAs in rice (Oryza sativa). J. Exp. Bot. 62, 3563–3573.

Diop, S.I., et al., 2020. A pseudomolecule-scale genome assembly of the liverwort Marchantia polymorpha. Plant J. 101, 1378–1396.

Dray, S., Dufour, A.-B., 2007. The ade4 package: implementing the duality diagram for ecologists. J. Stat. Softw. 22, 1–20.

Dubey, S., et al., 2020. Identification and expression analysis of conserved microRNAs during short and prolonged chromium stress in rice (Oryza sativa). Environ. Sci. Pollut. Res. 27, 380–390.

Elvira, N.J., Medina, N.G., Leo, M., Cala, V., Estébanez, B., 2020. Copper content and resistance mechanisms in the terrestrial moss ptychostomum capillare: a case study in an abandoned copper mine in Central Spain. Arch. Environ. Contam. Toxicol. 79, 49–59.

Ezaki, B., Higashi, A., Nanba, N., Nishiuchi, T., 2016. An S-adenosyl methionine synthetase (SAMS) gene from Andropogon virginicus L. Confers aluminum stress tolerance and facilitates epigenetic gene regulation in Arabidopsis thaliana. Front. Plant Sci. 7, 1627.

Feng, H., Conneely, K.N., Wu, H., 2014. A Bayesian hierarchical model to detect differentially methylated loci from single nucleotide resolution sequencing data. Nucleic Acids Res. 42, e69.

Feng, S.J., et al., 2020. Identification of epigenetic mechanisms in paddy crop associated with lowering environmentally related cadmium risks to food safety. Environ. Pollut. 256, 113464.

Feng, S.J., Liu, X.S., Cao, H.W., Yang, Z.M., 2021. Identification of a rice metallochaperone for cadmium tolerance by an epigenetic mechanism and potential use for clean up in wetland. Environ. Pollut. 288, 117837.

Filek, M., et al., 2008. The protective role of selenium in rape seedlings subjected to cadmium stress. J. Plant Physiol. 165, 833–844.

Fu, L., Niu, B., Zhu, Z., Wu, S., Li, W., 2012. CD-HIT: accelerated for clustering the next-generation sequencing data. Bioinformatics 28, 3150–3152.

Galati, S., et al., 2021. Heavy metals modulate DNA compaction and methylation at CpG sites in the metal hyperaccumulator Arabidopsis halleri. Environ. Mol. Mutagen. 62, 133–142.

Gao, J., Sun, L., Yang, X., Liu, J.-X., 2013. Transcriptomic analysis of cadmium stress response in the heavy metal hyperaccumulator sedum alfredii Hance. PLoS One 8, e64643.

Gehring, M., Bubb, K.L., Henikoff, S., 2009. Extensive demethylation of repetitive elements during seed development underlies gene imprinting. Science 324, 1447–1451.

Ghosh, I., Sadhu, A., Moriyasu, Y., Bandyopadhyay, M., Mukherjee, A., 2019. Manganese oxide nanoparticles induce genotoxicity and DNA hypomethylation in the moss Physcomitrella patens. Mutat. Res. Genet. Toxicol. Environ. Mutagen. 842, 146–157.

Götz, S., et al., 2008. High-throughput functional annotation and data mining with the Blast2GO suite. Nucleic Acids Res. 36, 3420–3435.

Goudet, J., 2005. hierfstat, a package for r to compute and test hierarchical F-statistics. Mol. Ecol. Notes 5, 184–186.

Grabherr, M.G., et al., 2011. Full-length transcriptome assembly from RNA-Seq data without a reference genome. Nat. Biotechnol. 29, 644–652.

Greco, M., Chiappetta, A., Bruno, L., Bitonti, M.B., 2012. In Posidonia oceanica cadmium induces changes in DNA methylation and chromatin patterning. J. Exp. Bot. 63, 695–709.

Gullì, M., Marchi, L., Fragni, R., Buschini, A., Visioli, G., 2018. Epigenetic modifications preserve the hyperaccumulator Noccaea caerulescens from Ni geno-toxicity. Environ. Mol. Mutagen. 59, 464–475.

Guschina, I.A., Harwood, J.L., 2002. Lipid metabolism in the moss Rhytidiadelphus squarrosus (Hedw.) Warnst. from lead-contaminated and non-contaminated populations. J. Exp. Bot. 53, 455–463.

Haas, B.J., et al., 2013. De novo transcript sequence reconstruction from RNA-seq using the Trinity platform for reference generation and analysis. Nat. Protoc. 8, 1494–1512.

Halimaa, P., et al., 2014. Gene expression differences between *Noccaea caerulescens* ecotypes help to identify candidate genes for metal phytoremediation. Environ. Sci. Technol. 48, 3344–3353.

Hanikenne, M., et al., 2008. Evolution of metal hyperaccumulation required cis-regulatory changes and triplication of HMA4. Nature 453, 391–395.

Hasan, M.K., et al., 2017. Responses of PLant Proteins to Heavy Metal Stress—a Review. Front. Plant Sci. 8.

He, Z.L., Yang, X.E., Stoffella, P.J., 2005. Trace elements in agroecosystems and impacts on the environment. J. Trace Elem. Med. Biol. 19, 125–140.

Hellwege, E.M., Dietz, K.-J., Volk, O.H., Hartung, W., 1994. Abscisic acid and the induction of desiccation tolerance in the extremely xerophilic liverwort Exormotheca holstii. Planta 194, 525–531.

Herrera, C.M., Bazaga, P., 2013. Epigenetic correlates of plant phenotypic plasticity: DNA methylation differs between prickly and nonprickly leaves in heterophyllous Ilex aquifolium (Aquifoliaceae) trees. Bot. J. Linn. Soc. 171, 441–452.

Huang, S.Q., et al., 2010. A set of miRNAs from Brassica napus in response to sulphate deficiency and cadmium stress. Plant Biotechnol. J. 8, 887–899.

Huang, S.Q., Peng, J., Qiu, C.X., Yang, Z.M., 2009. Heavy metal-regulated new microRNAs from rice. J. Inorg. Biochem. 103, 282–287.

Huerta-Cepas, J., et al., 2019. eggNOG 5.0: a hierarchical, functionally and phylogenetically annotated orthology resource based on 5090 organisms and 2502 viruses. Nucleic Acids Res. 47, D309–D314.

Hussain, A., Nazir, F., Fariduddin, Q., 2019. Polyamines (spermidine and putrescine) mitigate the adverse effects of manganese induced toxicity through improved antioxidant system and photosynthetic attributes in Brassica juncea. Chemosphere 236, 124830.

Janicka-Russak, M., Kabała, K., Burzyński, M., Kłobus, G., 2008. Response of plasma membrane H+-ATPase to heavy metal stress in Cucumis sativus roots. J. Exp. Bot. 59, 3721–3728.

Jombart, T., 2008. adegenet: a R package for the multivariate analysis of genetic markers. Bioinformatics 24, 1403–1405.

Kamvar, Z.N., Tabima, J.F., Grünwald, N.J., 2014. Poppr: an R package for genetic analysis of populations with clonal, partially clonal, and/or sexual reproduction. PeerJ 2, e281.

Kanawade, S.M., Hamigi, A.D., Gaikwad, R.W., 2010. Ecological effect of pollution. IJCEA 332–335. https://doi.org/10.7763/IJCEA.2010.V1.57.

Kawa, D., Testerink, C., 2017. Regulation of mRNA decay in plant responses to salt and osmotic stress. Cell Mol. Life Sci. 74, 1165–1176.

Kent, W.J., 2002. BLAT—the BLAST-like alignment tool. Genome Res. 12, 656–664.

Konno, H., Nakashima, S., Katoh, K., 2010. Metal-tolerant moss Scopelophila cataractae accumulates copper in the cell wall pectin of the protonema. J. Plant Physiol. 167, 358–364.
Krämer, U., 2010. Metal hyperaccumulation in plants. Annu. Rev. Plant Biol. 61, 517–534.
Krzesłowska, M., Woźny, A., 2008. Lead uptake, localization and changes in cell ultrastructure ofFunaria hygrometrica protonemata. Biol. Plant. https://doi.org/10.1007/BF02873855.
Krzesłowska, M., Lenartowska, M., Mellerowicz, E.J., Samardakiewicz, S., Woźny, A., 2009. Pectinous cell wall thickenings formation—a response of moss protonemata cells to lead. Environ. Exp. Bot. 65, 119–131.
Kumar, M., Bijo, A.J., Baghel, R.S., Reddy, C.R.K., Jha, B., 2012. Selenium and spermine alleviate cadmium induced toxicity in the red seaweed Gracilaria dura by regulating antioxidants and DNA methylation. Plant Physiol. Biochem. 51, 129–138.
Küpper, H., Šetlík, I., Spiller, M., Küpper, F.C., Prášil, O., 2002. Heavy metal-induced inhibition of photosynthesis: targets of in vivo heavy metal chlorophyll formation1. J. Phycol. 38, 429–441.
Küpper, H., Dědic, R., Svoboda, A., Hála, J., Kroneck, P.M.H., 2002. Kinetics and efficiency of excitation energy transfer from chlorophylls, their heavy metal-substituted derivatives, and pheophytins to singlet oxygen. Biochim. Et. Biophys. Acta (BBA) Gen. Subj. 1572, 107–113.
Lang, D., et al., 2018. The Physcomitrella patens chromosome-scale assembly reveals moss genome structure and evolution. Plant J. 93, 515–533.
Lang, I., Wernitznig, S., 2011. Sequestration at the cell wall and plasma membrane facilitates zinc tolerance in the moss Pohlia drummondii. Environ. Exp. Bot. 74, 186–193.
Lang, Z., et al., 2017. Critical roles of DNA demethylation in the activation of ripening-induced genes and inhibition of ripening-repressed genes in tomato fruit. Proc. Natl. Acad. Sci. USA 114, E4511–E4519.
Langmead, B., Salzberg, S.L., 2012. Fast gapped-read alignment with Bowtie 2. Nat. Methods 9, 357–359.
Legendre, P., Anderson, M.J., 1999. Distance-based redundancy analysis: testing multispecies responses in multifactorial ecological experiments. Ecol. Monogr. 69, 1–24.
Lemire, J.A., Harrison, J.J., Turner, R.J., 2013. Antimicrobial activity of metals: mechanisms, molecular targets and applications. Nat. Rev. Microbiol 11, 371–384.
Li, B., Dewey, C.N., 2011. RSEM: accurate transcript quantification from RNA-Seq data with or without a reference genome. BMC Bioinforma. 12, 323.
Li, B., Carey, M., Workman, J.L., 2007. The role of chromatin during transcription. Cell 128, 707–719.
Medrano, M., Herrera, C.M., Bazaga, P., 2014. Epigenetic variation predicts regional and local intraspecific functional diversity in a perennial herb. Mol. Ecol. 23, 4926–4938.
Mehdi, S., et al., 2016. The WD40 domain protein MSI1 functions in a histone deacetylase complex to fine-tune abscisic acid signaling. Plant Cell 28, 42–54.
Meier, S.K., et al., 2018. Comparative RNA-seq analysis of nickel hyperaccumulating and non-accumulating populations of Senecio coronatus (Asteraceae). Plant J. 95, 1023–1038.
Mounger, J., et al., 2021. Inheritance of DNA methylation differences in the mangrove Rhizophora mangle. Evol. Dev. 23, 351–374.
Nahar, K., Hasanuzzaman, M., Suzuki, T., Fujita, M., 2017. Polyamines-induced aluminum tolerance in mung bean: a study on antioxidant defense and methylglyoxal detoxification systems. Ecotoxicology 26, 58–73.
Niedziela, A., 2018. The influence of Al3+ on DNA methylation and sequence changes in the triticale (× Triticosecale Wittmack) genome. J. Appl. Genet. 59, 405–417.
Nomura, T., Hasezawa, S., 2011. Regulation of gemma formation in the copper moss Scopelophila cataractae by environmental copper concentrations. J. Plant Res 124, 631–638.
Oksanen, J. et al. vegan: Community Ecology Package. (2020).
OmicsBox – Bioinformatics Made Easy , BioBam Bioinformatics, March 3, 2019,. (2019).
Ou, X., et al., 2012. Transgenerational inheritance of modified DNA methylation patterns and enhanced tolerance induced by heavy metal stress in rice (Oryza sativa L.). PLOS ONE 7, e41143.
Papadopulos, A.S.T., et al., 2021. Rapid parallel adaptation to anthropogenic heavy metal pollution. Mol. Biol. Evol. 38, 3724–3736.
Park, Y., Wu, H., 2016. Differential methylation analysis for BS-seq data under general experimental design. Bioinformatics 32, 1446–1453.
Patanun, O., et al., 2017. The histone deacetylase inhibitor suberoylanilide hydroxamic acid alleviates salinity stress in cassava. Front. Plant Sci. 7.
Pence, N.S., et al., 2000. The molecular physiology of heavy metal transport in the Zn/Cd hyperaccumulator Thlaspi caerulescens. PNAS 97, 4956–4960.
Pence, V.C., 1998. Cryopreservation of bryophytes: the effects of abscisic acid and encapsulation dehydration. Bryologist 101, 278–281.
Petraglia, A., et al., 2014. The capability to synthesize phytochelatins and the presence of constitutive and functional phytochelatin synthases are ancestral (plesiomorphic) characters for basal land plants. J. Exp. Bot. 65, 1153–1163.
Platt, A., Gugger, P.F., Pellegrini, M., Sork, V.L., 2015. Genome-wide signature of local adaptation linked to variable CpG methylation in oak populations. Mol. Ecol. 24, 3823–3830.
Pour, A.H., Özkan, G., Nalci, Ö.B., HalilLoğlu, K., 2019. Estimation of genomic instability and DNA methylation due to aluminum (Al) stress in wheat (Triticum aestivum L.) using iPBS and CRED-iPBS analyses. Turk. J. Bot. 43, 27–37.
Puy, J., et al., 2021. Competition-induced transgenerational plasticity influences competitive interactions and leaf decomposition of offspring. N. Phytol. 229, 3497–3507.
Rahavi, M.R., Migicovsky, Z., Titov, V., Kovalchuk, I., 2011. Transgenerational Adaptation to Heavy Metal Salts in Arabidopsis. Front Plant Sci. 2.
Rathore, P., Raina, S.N., Kumar, S., Bhat, V., 2020. Retro-element gypsy-163 is differentially methylated in reproductive tissues of apomictic and sexual plants of Cenchrus ciliaris. Front. Genet. 11, 795.
Rhind, S.M., 2009. Anthropogenic pollutants: a threat to ecosystem sustainability? Philos. Trans. R. Soc. Lond. B Biol. Sci. 364, 3391–3401.
Richards, C.L. & Pigliucci, M. Epigenetic Inheritance. A Decade into the Extended Evolutionary Synthesis. PG (2020) doi:10.30460/99624.
Robertson, M. et al. Combining epiGBS markers with long read transcriptome sequencing to assess differentiation associated with habitat in Reynoutria (aka Fallopia). 2020.09.30.317966 (https://www.biorxiv.org/content/10.1101/2020.09.30.317966v1) (2020) doi:10.1101/2020.09.30.317966.
Robinson, M.D., McCarthy, D.J., Smyth, G.K., 2010. edgeR: a Bioconductor package for differential expression analysis of digital gene expression data. Bioinformatics 26, 139–140.
Róis, A.S., et al., 2013. Epigenetic rather than genetic factors may explain phenotypic divergence between coastal populations of diploid and tetraploid Limonium spp. (Plumbaginaceae) in Portugal. BMC Plant Biol. 13, 205.
RStudio Team. RStudio: Integrated Development for R. RStudio, PBC, Boston, MA. (2019).
Sabovljević, M.S., et al., 2020. Metal accumulation in the acrocarp moss Atrichum undulatum under controlled conditions. Environ. Pollut. 256, 113397.
Sanchez, D.H., Paszkowski, J., 2014. Heat-induced release of epigenetic silencing reveals the concealed role of an imprinted plant gene. PLOS Genet. 10, e1004806.
Sarry, J.-E., et al., 2006. The early responses of Arabidopsis thaliana cells to cadmium exposure explored by protein and metabolite profiling analyses. PROTEOMICS 6, 2180–2198.
Schmid, M.W., et al., 2018. Extensive epigenetic reprogramming during the life cycle of Marchantia polymorpha. Genome Biol. 19, 9.
Shafiq, S., et al., 2019. Lead, Cadmium and Zinc Phytotoxicity Alter DNA Methylation Levels to Confer Heavy Metal Tolerance in Wheat. Int J. Mol. Sci. 20.
Shahid, M., et al., 2014. Heavy-Metal-Induced Reactive Oxygen Species: Phytotoxicity and Physicochemical Changes in Plants. In: Whitacre, D.M. (Ed.), in Reviews of Environmental Contamination and Toxicology, Volume 232. Springer International Publishing, pp. 1–44. https://doi.org/10.1007/978-3-319-06746-9_1.
Shaw, A.J., 1993a. Population biology of the rare copper moss, Scopelophila cataractae. Am. J. Bot. 80, 1034–1041. https://doi.org/10.2307/2445751.
Shaw, A.J., 1993b. Morphological uniformity among widely disjunct populations of the rare 'Copper Moss,' Scopelophila cataractae (Pottiaceae). Syst. Bot. 18, 525–537. https://doi.org/10.2307/2419424.
Shaw, A.J., 1995. Genetic biogeography of the rate 'copper moss', Scopelophila cataractae (Pottiaceae). Plant Syst. Evol. 197, 43–58.
Shaw, J., 1987. Evolution of heavy metal tolerance in bryophytes. II. An ecological and experimental investigation of the 'Copper Moss,' Scopelophila cataractae (Pottiaceae). Am. J. Bot. 74, 813–821.
Shaw, J., 1989. Heavy Metal Tolerance in. Plants: Evolutionary Aspects. CRC Press.
Simão, F.A., Waterhouse, R.M., Ioannidis, P., Kriventseva, E.V., Zdobnov, E.M., 2015. BUSCO: assessing genome assembly and annotation completeness with single-copy orthologs. Bioinformatics 31, 3210–3212.
Simms, E.L., 2000. Defining tolerance as a norm of reaction. Evolut. Ecol. 14, 563–570.
Smit, A., Hubley, R., Green, P., 2013. RepeatMasker Open 4, 0.
Stark, L.R., Brinda, J.C., Nicholas McLetchie, D., Oliver, M.J., 2012. Extended periods of hydration do not elicit dehardening to desiccation tolerance in regeneration trials of the moss Syntrichia caninervis. Int. J. Plant Sci. 173, 333–343.
Talke, I.N., Hanikenne, M., Krämer, U., 2006. Zinc-dependent global transcriptional control, transcriptional deregulation, and higher gene copy number for genes in metal homeostasis of the Hyperaccumulator Arabidopsis halleri. Plant Physiol. 142, 148–167.
Tamás, M.J., Sharma, S.K., Ibstedt, S., Jacobson, T., Christen, P., 2014. Heavy metals and metalloids as a cause for protein misfolding and aggregation. Biomolecules 4, 252–267.
Tan, Y.-F., O'Toole, N., Taylor, N.L., Millar, A.H., 2010. Divalent metal ions in plant mitochondria and their role in interactions with proteins and oxidative stress-induced damage to respiratory function. Plant Physiol. 152, 747–761.
Taspinar, M.S., et al., 2018. Aluminum-induced changes on DNA damage, DNA methylation and LTR retrotransposon polymorphism in maize. Arab J. Sci. Eng. 43, 123–131.
Tsuji, H., Saika, H., Tsutsumi, N., Hirai, A., Nakazono, M., 2006. Dynamic and reversible changes in histone H3-Lys4 Methylation and H3 acetylation occurring at submergence-inducible genes in rice. Plant Cell Physiol. 47, 995–1003.
van de Mortel, J.E., et al., 2006. Large expression differences in genes for iron and zinc homeostasis, stress response, and lignin biosynthesis distinguish roots of arabidopsis thaliana and the related metal hyperaccumulator Thlaspi caerulescens. Plant Physiol. 142, 1127–1147.
van Gurp, T.P., et al., 2016. epiGBS: reference-free reduced representation bisulfite sequencing. Nat. Methods 13, 322–324.
Verbruggen, N., Hermans, C., Schat, H., 2009. Molecular mechanisms of metal hyperaccumulation in plants. N. Phytol. 181, 759–776.
Verhoeven, K.J.F., Jansen, J.J., van Dijk, P.J., Biere, A., 2010. Stress-induced DNA methylation changes and their heritability in asexual dandelions. N. Phytol. 185, 1108–1118.
Wang, X., Shi, G., Xu, Q., Hu, J., 2007. Exogenous polyamines enhance copper tolerance of Nymphoides peltatum. J. Plant Physiol. 164, 1062–1070.
Wang, Y., Qian, M., Ruan, P., Teschendorff, A.E., Wang, S., 2019. Detection of epigenetic field defects using a weighted epigenetic distance-based method. e6–e6 Nucleic Acids Res. 47. e6–e6.

Xie, F.L., et al., 2007. Computational identification of novel microRNAs and targets in Brassica napus. FEBS Lett. 581, 1464–1474.
Xin, C., Chi, J., Zhao, Y., He, Y., Guo, J., 2019. Cadmium stress alters cytosine methylation status and expression of a select set of genes in Nicotiana benthamiana. Plant Sci. 284, 16–24.
Yadav, N.S. et al. Multigenerational exposure to heat stress induces phenotypic resilience, and genetic and epigenetic variations in Arabidopsis thaliana offspring. 2020.11.30.405365 ⟨https://www.biorxiv.org/content/10.1101/2020.11.30.405365v1⟩ (2020) doi:10.1101/2020.11.30.405365.
Zemach, A., McDaniel, I.E., Silva, P., Zilberman, D., 2010. Genome-wide evolutionary analysis of eukaryotic DNA methylation. Science.
Zhang, M., Xu, C., von Wettstein, D., Liu, B., 2011. Tissue-specific differences in cytosine methylation and their association with differential gene expression in Sorghum1[W]. Plant Physiol. 156, 1955–1966.
Zheng, X., Zhang, N., Wu, H.-J., Wu, H., 2017. Estimating and accounting for tumor purity in the analysis of DNA methylation data from cancer studies. Genome Biol. 18, 17.
Zhou, Z.S., Huang, S.Q., Yang, Z.M., 2008. Bioinformatic identification and expression analysis of new microRNAs from Medicago truncatula. Biochem. Biophys. Res. Commun. 374, 538–542.